Wideband Radio Frequency Interference Cancellation for High-sensitivity Phased Array Receivers with True Time Delays and Truncated Hadamard Projection

Jakob W. Kunzler, Member, IEEE, Karl F. Warnick, Fellow, IEEE

Abstract—Radio frequency interference (RFI) is a significant challenge for high-sensitivity phased array instruments. RFI can be suppressed using digital signal processing, but to improve dynamic range for wideband RFI, it can be desirable to remove interference in the analog domain before sampling. In previous work, it has been shown that analog true time delay (TTD) stages with a truncated Hadamard transform can place a wide-band spatial null on RFI from a given direction of arrival. We show that TTD and Hadamard projection is mathematically equivalent to a bank of classical narrow-band subspace projection beamformers, but with a structure that allows efficient implementation in either analog circuitry or digital hardware. We analyze how loss in the TTD blocks and time delay errors affect beamformer performance and propose methods for calibrating time delays. Simulation results show that ideal TTD and Hadamard projection matches the bank of subspace projection beamformers and places deep nulls over wideband RFI signals while achieving SNR performance comparable to the maximum signal to interference and noise ratio beamformer.

Index Terms—Phased arrays, Time-delay arrays, Hadamard transforms, Interference suppression

I. INTRODUCTION

Radio frequency interference (RFI) is a serious problem for passive spectrum users in remote sensing and radio astronomy. Time and frequency blanking, beam pattern nulling and spatial filtering, adaptive filters, and many other methods have been used for RFI mitigation [1], [2]. Traditional digital RFI mitigation schemes for phased arrays such as maximum signal to interference and noise beamforming and subspace projection [1] are inherently narrow band, and are implemented for wideband signals using a fast Fourier transform or polyphase filterbank after sampling. The interferer must be identified and canceled separately in each subband, leading to significant computational overhead for real time signal processing receivers. Analog phase shift beamforming does not require real time digital computation to cancel RFI, but is also limited to narrow band signals and does easily allow computing many beams in parallel. It would be desirable if there were a compromise between the two architectures that could implement a wideband RFI cancellation beamformer in analog while preserving signals of interest for filtering by downstream digital beamformers.

Department of Electrical and Computer Engineering, Brigham Young University, Provo, Utah, 84602, USA e-mail: jake.kunzler@gmail.com

This material is based upon work supported by the National Science Foundation under Grant Nos. 2030165 and 2030159

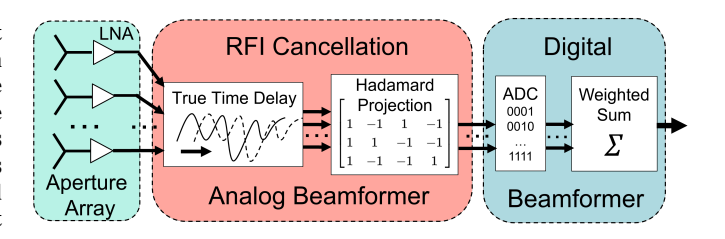


Fig. 1. The TTD and Hadamard projection method remove RFI before conventional beamforming. With placement in analog, it can protect the dynamic range of high sensitivity receivers against RFI. This architecture is the analog implementation of computing a bank of narrow band subspace projection beamformers.

To cancel RFI from a single fixed position, line of sight, wideband source, Ghaderi et al.[3] introduced a true timedelay (TTD) and truncated Hadamard projection operator method. Accompanying this method, they have produced a TTD chip prototype that achieves 5 ps of resolution over 100 MHz at baseband [4]. Pending good implementation of TTD, this algorithm is inherently broadband for canceling line-of-sight interferers. The matrix transform preserves the ability for downstream beamformers to perform second stage synthesis imaging around the null pattern produced by time delayed Hadamard projection. This algorithm is convenient to both analog and digital implementations. The analog implementation can reduce the computational complexity of real time RFI mitigation and protect the receiver's dynamic range from strong RFI incursions.

Hadamard matrices have been explored for many applications in numerical and statistical analysis [5]. Perhaps the most familiar application is error correcting Hadamard codes [6]. Broadcasting Hadamard coded modulations have been used for decreasing signal to interference ratio in phased array radars [7] and improving SNR in phased array imaging [8]. The common mode isolation property of the Hadamard transform has been explored for use in simultaneous wireless information and power transfer by extracting DC power embedded in communication waveforms [9]. Others work has investigated Hadamard antenna feeding networks for forming dual concurrent beams in a phased array [10]. This paper builds on [11] in exploring the application of the Hadamard transform to phased array antennas.

The goal here is to extend the TTD and truncated Hadamard

TABLE I
COMPARISON OF INTERFERENCE CANCELLATION ALGORITHMS

Comparing Interference Cancellation Algorithms		
Method	Pros	Cons
Analog Phase Shifters	No computational cost RFI reduced before sampling	Costly components Narrow band Cannot cascade
Bank of Digital Max SINR	· Optimal balance between signal, noise, and interference	Requires port correlations for each signal component Computationally expensive Not zero forcing
Bank of Digital Subspace Projection	· Zero forcing null for RFI	Requires RFI subspace estimation Computationally expensive
Analog TTD + Hadamard Projection	Zero forcing null for RFI Native wideband Reduced computational cost RFI reduced before sampling Allows downstream beamformers	Requires TTD calibration. Analog stability issues

projection method to high-sensitivity phased array applications like radio astronomy, where the SNR of weak signals of interest can be -30 to -50 dB or lower. The target application for this technology is in the analog front-ends of high sensitivity arrays that are performance limited by RFI. The time delayed Hadamard projection sacrifices one array element degree of freedom to place a zero forcing wideband null over the offending RFI. After projection, the cleaned signal paths are fed downstream to a conventional digital beamforming architecture. The analog projection can protect downstream digitizers from being overdriven by strong interference. Table I summarizes the strengths and weaknesses of various interference cancellation techniques in comparison to time-delayed Hadamard projection.

We develop a theoretical basis for time delayed Hadamard projection by showing the analytical relationship to the bank of narrow-band subspace projection beamformers. Numerical simulations that confirm this analysis are presented. The simulations also indicate the expected beamformer performance. A study of how TTD imperfections relate to beam quality is offered. We propose two methods for calibrating the time delays for a given interfering source angle of arrival. Lastly, a brief discussion about the efficient all digital implementation of the algorithm is included.

II. WIDEBAND BEAMFORMING MODEL

Figure 1 shows the combined analog and digital beamformer architecture. The TTD stage is designed to create coherence for signals arriving in the direction of RFI. After time aligning the RFI, the RFI appears like a common mode bias to each port. The truncated Hadamard transform implements a projection matrix that removes the common mode bias among all ports to cancel the RFI. The result of removing the common mode is a zero-forcing condition imposed on all signals in the direction of the RFI. This projection operator sacrifices an output port to clean the RFI from the remaining data streams. The remaining

ports contain a mixture of all signals outside the null region of projection. These can be filtered by a secondary beamforming to select the signals of interest.

A. Analog Beamformer

The truncated Hadamard matrix is the traditional Hadamard matrix \mathbf{H} [5] sans the top row of ones. The notation \mathbf{H}_p is used to designate the rank deficiency that creates a projection step by discarding the top row. The matrix \mathbf{H}_p may be represented in N-1 by N truncated form or in square matrix form by filling the top row with zeros. The square form of this matrix is convenient for symbolic manipulation and is used in this paper. The length 4 truncated Hadamard matrix is

The loss in rank represents a projection from a full rank system to a system with a rank one null space. The null space of \mathbf{H}_p is the span of common mode signals shared by all the ports. The balanced number of ± 1 in the other rows means that shared signals common to each port are removed by the balanced additions and subtractions of the transform.

The square matrix definition of the projection operator can be viewed as a modification to the Hadamard transformation with its fast computational algorithm [5]. To model the square projection operator with the fast Hadamard transform, simply set the first element of the output vector to zero. This procedure is computationally efficient for simulating Hadamard projection on vectors of time domain waveforms.

The top row common mode port is discarded for theoretical derivation of the RFI cancellation beamformer, but it can have practical value that warrants maintaining the port's data. This port may be sampled for further use in characterizing the RFI in the digital signal processing assuming the coherent RFI does not saturate the dynamic range. This feature can be useful for calibrating the TTD weights (see Sec. IV-C). Another reason for maintaining the port is RFI leakage. A practical TTD device has discrete delay states that will not allow perfect zero-forcing of the RFI and some leakage through the projection will occur. The common mode port will have a strong estimate of the RFI time domain waveform and can be used for RFI subtraction later in the DSP.

A TTD circuit is one which implements the transformation $s(t) \to s(t-\tau)$ for some small time delay τ on some time domain waveform s(t). When implemented with an analog circuit at baseband, the local oscillator phase of the mixer must also be compensated in the down-conversion to preserve the correct phase relationship before the matrix summations. When a unique TTD is applied to n ports, the convention is the time lags are normalized such that the smallest time delay is defined as zero. The time delays for port n are dependent on array geometry, and are conventionally designed to align signals coherently from a given direction of arrival.

When using phasor analysis, the TTD transformation phasors can be stored in a column vector $\mathbf{d}[n] = \exp(j\omega\tau[n])$.

To apply the time delay to each port, define the matrix operator $\mathbf{D} = \operatorname{diag}\left(\mathbf{d}\right)$ as a diagonal matrix to apply the delay transformation to the array response vector \mathbf{v} . The array response vector $\mathbf{v}(f,\hat{p},\theta,\phi)$ is the column vector containing the collection of phasors observed at each port of a receiving antenna in an aperture array as a function of frequency f, polarization \hat{p} , and spherical incidence angles θ and ϕ . In RFI zero-forcing mode, the conjugate-field-match (CFM) constraint $\mathbf{d} = \mathbf{v}_{\text{RFI}}^*$ is applied across all frequencies of support. The vector of ideal TTD weights $\tau[n]$ is then given by the explicit formula

$$\tau[n] = \frac{-\arg \mathbf{v}[n]}{\omega} + b$$
 (2)
$$b: \tau[n] \ge 0 \ \forall \ n$$

where scalar b enforces causality in the delay weights.

With the notation established, it can be shown that time delayed Hadamard projection is an isomorphism of the subspace projection beamformer at each frequency. The subspace projection beamformer is defined by the matrix **P**

$$\mathbf{P} = \mathbf{I} - \frac{\mathbf{v}\mathbf{v}^{\mathrm{H}}}{N} = \mathbf{P}^{\mathrm{H}} \tag{3}$$

with null space equal to the span of exactly one array response vector \mathbf{v} such that $\mathbf{P}\mathbf{v} = \mathbf{0}$.

The Hadamard matrix is a full rank orthogonal matrix. Removing a row of the matrix by setting the row to 0 creates a new matrix with null space equal to the span of the removed row. The removed row for \mathbf{H}_p is 1, meaning the null space is the span of 1. Since \mathbf{v} is nonzero, there exists a diagonal matrix \mathbf{D} such that $\mathbf{1} = \mathbf{D}\mathbf{v}$. This is the conjugate-field-match constraint for every phasor frequency.

Since \mathbf{D} is diagonal (invertable), this implies the null space of the cancellation beamformer can be transformed into the exact array response vector \mathbf{v} . Since both approaches yield matrices with equivalent null spaces equal to the span of \mathbf{v} , they must be isomorphic projection operators related by some full rank rotation matrix \mathbf{F} . This implies the time delayed and Hadamard projection method is an isomorphism of the subspace projection beamformer through \mathbf{F} namely

$$\mathbf{FPv} = \mathbf{H}_{\mathbf{n}}\mathbf{D}\mathbf{v} = \mathbf{0} \tag{4}$$

The beam response pattern under a subspace projection operator \mathbf{P} for the original weighting vector \mathbf{w}_0 designed without \mathbf{P} is approximately preserved for all array response vectors outside a small neighborhood of the null space of \mathbf{P} via the transformation $\mathbf{w} = \mathbf{P}\mathbf{w}_0$. Symbolically, this is

$$v = \mathbf{w}_0^{\mathrm{H}} \mathbf{v} = \mathbf{w}_0^{\mathrm{H}} \mathbf{P} \mathbf{v} = \mathbf{w}^{\mathrm{H}} \mathbf{v}$$
 (5)

B. Digital Beamformer

Since power from array response vectors outside of the null is preserved, but rotated during the TTD, a secondary reconstruction beamformer is required to align the ports before a second coherent summation. That is, the reconstruction beamformer is required to restore coherence for the SOI direction after the projection step. The digital beamformer component contains the transformation $\mathbf{D}^H\mathbf{H}_p^H$ such that the

net result system is $\mathbf{D}^{\mathrm{H}}\mathbf{H}_{\mathrm{p}}^{\mathrm{H}}\mathbf{H}_{\mathrm{p}}\mathbf{D} \approx N^{2}\mathbf{I}$ where the approximation indicates a zero projection of some array response vector has occurred. The careful observer will recognize $\mathbf{H}_{\mathrm{p}}^{\mathrm{H}}$ could also be performed in analog hardware as well as \mathbf{D}^{H} with a second TTD stage, but this may be impractical.

Alternatively, many existing beamformer imaging technologies are implemented computationally across narrow frequency channels on sampled data for many pixels simultaneously. The architecture allow implementing of \mathbf{D}^H across each subchannel beamformer. This means that any beamforming weight vector \mathbf{w} designed for a system without the analog TTD and Hadamard projection hardware can be converted to work with the cancellation hardware by means of the transformation $\mathbf{w}^H \mathbf{D}^H \mathbf{H}_p^H$. The resulting beam will be close to the original beam with a null around the projected array response vector.

A large class of canonical beamformers are defined as optimizing solutions of generalized Rayleigh quotients of correlation matrices of array response vectors \mathbf{v} summed by beamformer weight vectors \mathbf{w} . The complex relationships between phasors are calculated with correlation matrices $\mathbf{R} = \mathbf{v}\mathbf{v}^H$ which are approximated as rank 1 structures. Array response vectors are used to represent the phase response of narrow-band channels due to incidence angle across the field of view. This leads to definitions of signal correlations for spatially localized signals-of-interest \mathbf{R}_S , interferers \mathbf{R}_I , and noise signals \mathbf{R}_N in the receiver. With these components, the maximum signal to interference and noise ratio beamformer is defined to maximize the expected power ratio of the SOI power to the combined interferer and noise powers. The definition is

$$w_{\text{maxSINR}} = \underset{w}{\text{arg max}} \ \frac{w^{\text{H}} R_{\text{S}} w}{w^{\text{H}} \left(R_{\text{N}} + R_{\text{I}} \right) w} \tag{6}$$

Quadratic form Rayleigh Quotient optimizations like this are analytically solved with the largest eigenvalue solution to the generalized eigenvalue problem $\mathbf{w}\mathbf{A} = \lambda \mathbf{w}\mathbf{B}$ where \mathbf{A} and \mathbf{B} are the top and bottom matrices between the vector products. This beamformer yields great success operating on digitally sampled data for emphasizing the antenna array response in the SOI direction and placing a spatial null over the interferer location (but is not a zero-forcing projection technique).

The correlation statistics in \mathbf{R} modified by linear transformation \mathbf{A} are $\mathbf{R}' = \mathbf{A}\mathbf{R}\mathbf{A}^{\mathrm{H}}$. The max SINR beamformer of (6) following time delayed Hadamard projection method is

$$w_{\text{max SNR, TTD + Hadamard}} = \underset{w}{\text{arg max}} \frac{w^{\text{H}} H_{\text{p}} D R_{\text{S}} D^{\text{H}} H_{\text{p}}^{\text{H}} w}{w^{\text{H}} H_{\text{p}} D R_{\text{N}} D^{\text{H}} H_{\text{p}}^{\text{H}} w}$$
(7)

The $\mathbf{R}_{\rm I}$ statistics are not included in the denominator because its rank one basis is the null space of $\mathbf{H}_p\mathbf{D}$. Equation (7) is the classical max SNR beamformer adapted to the signal and noise statistics after the zero-forcing RFI projection.

III. NUMERICAL RESULTS

The quality of the RFI cancellation and beam response can be computed with a simple numerical simulation. This is done by solving the beamformer weights \mathbf{w} for a target SOI and RFI direction, then evaluating the received power $\mathbf{w}^H \mathbf{R} \mathbf{w}$ where \mathbf{R} contains the appropriate array response vector correlations

for the pixel of interest due to transformations in the system model. Evaluating received power at pixels across the 3D field of view, then integrating for power, allows the power scan to be normalized for antenna directivity.

Modeling an isotropic noise field in an 8 x 8 receiver array spaced 0.5λ without mutual coupling, the directivity response of each beamformer can be evaluated in ideal conditions. The analog TTD and Hadamard projection method is assumed to have ideal TTD weights with perfect (double precision) resolution and all beamformers have perfect *a priori* knowledge of the array response vectors. The analog to digital conversion is modeled as perfect.

Figures 2 and 3 compare the beams from the various beamformers at three metric frequencies across the 310 MHz of analyzed bandwidth. The beams are tuned for a SOI at boresight with RFI at 10 degrees and 25 degrees θ along the ϕ axis at 45 degrees. For the red TTD + Hadamard curve, this response is due to the wideband TTD and Hadamard projection followed by a second stage digital max SINR beamformer applied in a narrow channel as given by (7). The other comparison digital beamformers, max SINR, max directivity, and subspace projection beamformer, are applied across narrow bands.

The maximum directivity beam indicates an optimized SNR beam without the presence of RFI. The maximum SINR beamformer is the optimization criteria of (6). The subspace projection beamformer from (3) puts a zero-forcing null over the RFI. As proven before, and demonstrated in these plots, the time delayed Hadamard projection obtains identical performance to the bank of narrow band subspace projection beamformers (with curves underneath barely visible). The zero-forcing constraint leads to slightly less control over side lobe ripple near the null compared to the max SINR beamformer, but still obtains good overall side-lobe control and main-lobe shape.

The SINR figure of merit can be used to quantify the quality of the RFI rejection across the field of view. The available SINR under different beamformer algorithms across the field of view is portrayed in Figure 4. This shows the obtained SINR under beamformer weights trained to observe each angular location in the presence of fixed RFI. The distance from the max directivity curve represents restored observation space from beamforming. The time delay Hadamard projection restores almost the same amount of observation space as the optimal max SINR beamformer.

IV. PRACTICAL CONSIDERATIONS

This paper has demonstrated that ideal TTD and a perfect Hadamard matrix implementation are identical to a bank of narrow band subspace projection beamformers. Real analog components will have confounding factors such as loss, variations in physical TTD applied, drift in the calibration settings, finite bandwidth in the TTD stages, unequal balancing in the Hadamard ports, and overall uncertainty in the performance of the analog chain. In general, all of these factors will reduce the effectiveness of the proposed method. This section gives a few studies to help quantify the loss in performance due

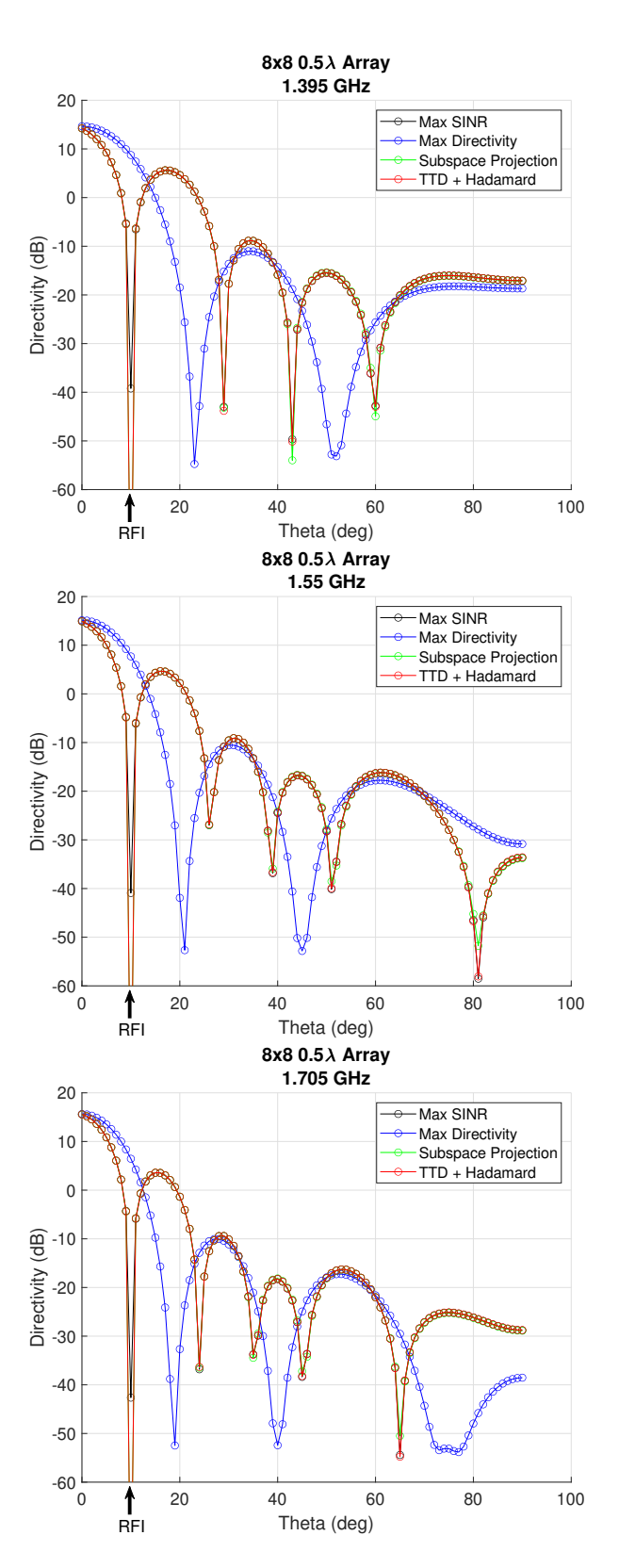


Fig. 2. Comparing the wideband TTD + Hadamard beamformer to other narrow band digital beamformers with RFI along the 45 degree plane. The SOI is at boresight and the RFI location is marked with the arrow. The analog TTD + Hadamard projection is applied wideband with secondary beamformer implemented narrow band.

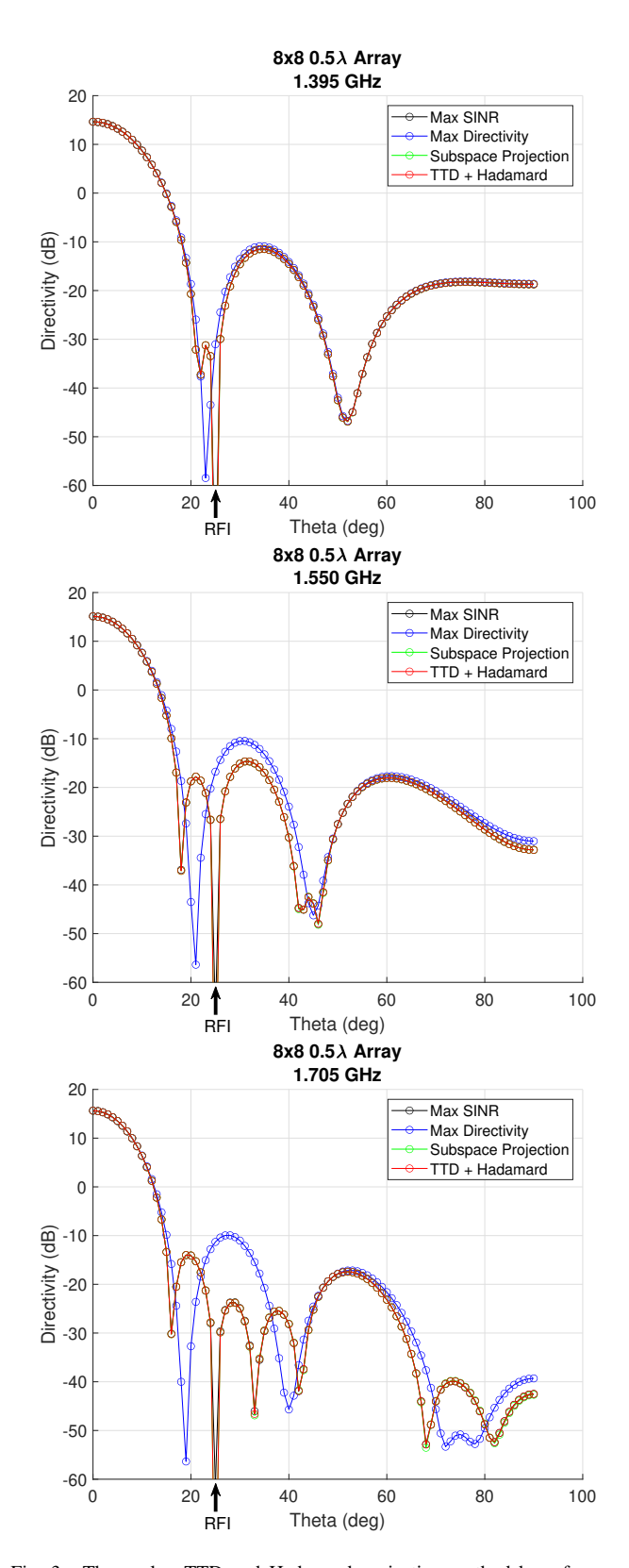


Fig. 3. The analog TTD and Hadamard projection method beamformer of (7) is practically identical to the digital subspace projection beamformer of (3) and very close to the digital maximum SINR beamformer of (6). The blue maximum directivity beamformer provides a reference by showing the optimization criteria for SNR without RFI.

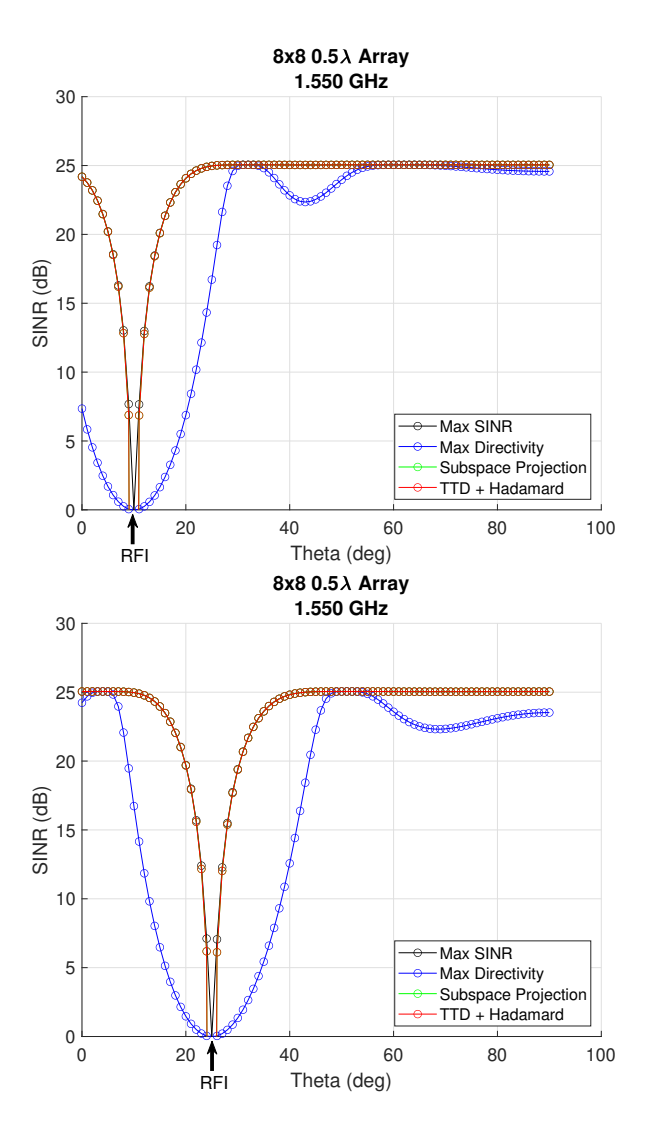


Fig. 4. The SINR map over scan angles of the main beam. The scanned SINR performance of the analog TTD and Hadamard projection method is identical to the subspace projection beamformer and nearly identical to the max SINR beamformer. The difference between the red and blue curves show the recoverable synthesis imaging space around the null by utilizing the analog TTD and Hadamard projection method. Only 1.550 GHz SINR scans are shown because they are typical of the 1.395 and 1.705 GHz behavior.

to imperfect TTD technology. If the imperfections associated with analog performance are found to be unacceptable for a given application, the reader may consider an all digital implementation of the algorithm discussed briefly in the last section.

A. Effect of Loss

Losses introduced by the analog front-end impact the system noise temperature and sensitivity of the array receiver. The signal loss caused by time delayed Hadamard projection occurs after amplification by first stage low noise amplifiers. If the gain and noise budget of the front end analog signal chains before the time delay circuit is properly designed, loss in the TTD and Hadamard components will have a negligible effect on the system noise temperature and sensitivity. The dynamic range of the front end receiver must be adequate to handle RFI before it is removed in the Hadamard block.

Unbalanced loss between adjacent receiver chains is different. It manifests as a distorting signal through the Hadamard projection that requires filtering by the downstream beamformer. To illustrate, consider an array response vector \mathbf{v} corresponding to an undesirable RFI source. Let unbalanced losses be modeled by perturbation of the array response vector by the vector \mathbf{g} . After applying the TTD tuned to \mathbf{v} and the Hadamard projection operator there will be a remaining signal $\mathbf{H}_p\mathbf{D}(\mathbf{v}+\mathbf{g})=\mathbf{H}_p\mathbf{D}\mathbf{g}$. This signal is only zero when \mathbf{g} is filled with the same value. The beamformer filters all components of \mathbf{g} that are common to each port and passes the variations downstream. The variation signal is rank 1, and the downstream beamformer will need to adjust to remove it. This will impact the quality of obtainable beam patterns depended the orthogonality of \mathbf{g} with the SOI array response vector.

Unequal balancing inside the Hadamard projection operator can manifest as a higher rank signal distortion. Consider the case where each element of \mathbf{H}_p were perturbed by a complex random matrix \mathbf{G} filled with independent terms taken from a circularly symmetric Gaussian distribution with variance σ^2 . An indicator of lost orthogonality between ports can be seen in the off-diagonal terms of the matrix $\mathbf{R} = (\mathbf{H} + \mathbf{G})^{\mathrm{H}}(\mathbf{H} + \mathbf{G})$. The proportional amount of power leaked from the common mode port into the other ports can be estimated by the ratio r of the average magnitude in the off diagonal terms of \mathbf{R} to the average magnitude along the diagonal of \mathbf{R} . After studying numerical sweeps of N and σ , this ratio is approximately given by the empirical expression $r = \sigma/\sqrt{N}$. For example, let $\sigma = 0.1$ (10% standard deviation), with N = 64 antennas, the percent of common mode leakage is about r = 1.25%.

B. Limited Time Delay Resolution

The analog RFI cancellation can be proven to work exactly with perfect resolution TTD stages and exact *a priori* array response vectors. In practice, quantized TTD states introduce rounding errors that tend to relax the zero-forcing null depth. The TTD weight quantization effect was estimated with a numerical simulation of the same 64 element array with a null at 10 degrees θ .

Figure 5 shows how TTD resolution affects interference rejection and SNR across bandwidth. These metrics are computed on the same beam as Figure 2. The left scale shows the interference rejection ratio (IRR) which is the interference to noise ratio (INR) out of the Hadamard projection on all ports divided by the INR of the strongest INR port on the input. This quantity is related to null depth. The IRR is linear in log scale with the precision of the TTD weights. This shows how an increasingly perfect TTD approaches the zero forcing condition that yields an infinitely deep null.

The right scale shows array gain for the signal of interest. Array gain is defined to be the SNR at the output ports divided by the SNR at one input port. RFI power is not included in array gain. For 64 elements, the array gain is expected to be $10\log_{10}(64)=18.06$ dB. Achieving less array gain than this curve indicates SNR loss across the bandwidth of the beamformer. The TTD and Hadamard projection shows less than 1 dB of SNR loss. This loss is identical to that

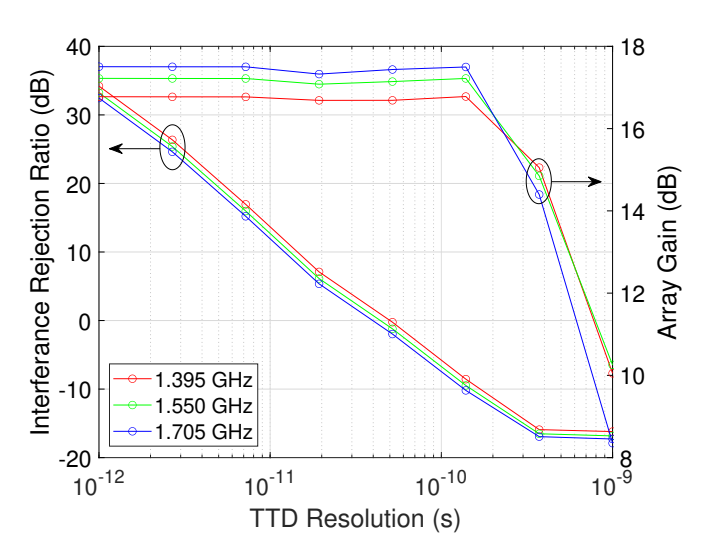


Fig. 5. Array gain and interferance rejection ratio vs TTD resolution for the beam in Figure

2. The resolution of TTD directly influences null depth across bandwidth (left scale) while providing consistent array gain (right scale) given sufficient TTD precision. The array gain within 1 dB of the limit of 18.06 dB is typical of a bank of subspace projection beamformers.

the loss of a bank of narrow band digital subspace projection beamformers. The plot show how the array gain saturates as once a sufficient amount of TTD resolution is applied.

Using the Hadamard projection, there will always be some loss in the array gain because the common mode port is discarded and N-1 ports are left for beamforming. This predicts that loss in array gain will always be at least $10\log_{10}\left[(N-1)/N\right]$ dB. For N = 64, this value is -0.068 dB. This bound is often exceeded by subspace projection beamformers because degrees of freedom are allocated to zero forcing then null depth and the expense of main lobe quality.

C. Time Delay Calibration

Physical circuits have many confounding factors that make exact calculation of the array response vectors uncertain. Both sources of error require a calibration procedure to estimate optimal TTD weights to force the RFI as low as possible. Two calibration algorithms for determining the TTD weighting vectors are proposed here. Both algorithms rely on the assumption that the RFI is significantly stronger than the signal of interest. These approaches utilize all of the ports of a full Hadamard transform including the common mode top row. This gives a compelling reason to maintain the full Hadamard transformation with the top common mode row in the analog circuitry when the dynamic range of the analog to digital conversion allows.

1) Power Ratio Heuristic Search: A feedback loop is used with a heuristic problem solver to seek a solution that minimizes the ratio of interferance power to signal of interest power. If the RFI power is strong, the optimization space should be highly convex and amenable to quasi-gradient techniques.

- Sample data emerging from all the ports of the full rank Hadamard transform.
- 2) Integrate the power observed from the top row common mode port. Call this P_1 .
- 3) Integrate the power observed from all other rows. Call this P_2 .
- 4) Apply a heuristic search such as simulated annealing or a genetic algorithm to methodically seek TTD weights that minimize the observed ratio P_2/P_1 . Minimizing this ratio forces the TTD stages to align with to the strong RFI.
- 2) Steering Vector Estimation: This technique is based on (4) and (2). It seeks weights that cancel the dominant array response vector of the received signal.
 - 1) Let the $N \times M$ matrix **V** represent M discrete time voltage signals from N antennas.
 - Reset the TTD weights to bypass mode (common delay)
 D = I.
 - 3) Sample the ADC voltages and time filter the ADC codes with a mixer and baseband filter operator F_{ω} on each time series for a narrow frequency channel ω of interest. Call these baseband voltages the matrix $\mathbf{V}_{\omega} = F_{\omega}(\mathbf{IHV})$.
 - 4) Compute the sample port correlation matrix of the baseband voltages ${\bf R}={\bf V}_\omega{\bf V}_\omega^{\ {\rm H}}.$
 - 5) Select the largest eigenvector **s** from the eigenvector decomposition of **R**.
 - 6) Now the estimated TTD weights should be set $\tau[n] = -\omega^{-1}\arg{(\mathbf{s})} + b$ following the definition in (2). These weights should now cancel the dominant RFI array response vector.

Figure 6 shows directivity patterns obtained on the same array after using a numerical simulation of each calibration strategy to estimate the TTD weights. The power ratio heuristic search is less robust in convergence than the steering vector estimator. The residual error from the estimation tends to relax the null depth and raise the side lobe levels compared to the ideal subspace projection (time delayed Hadamard) beamformer.

D. Combined Analog and Digital Cancellation

The role of analog time delayed Hadamard projection method is to place wideband response nulls before the digital signal processing. This frees up computational power in the digital domain for other operations, such as suppressing residual narrow band interference.

As analog to digital converter (ADC) technology continues to improve in sample rate and resolution, wide-dynamic range cancellation may become more practical in the digital domain. With finite time delay resolution, some RFI will leak through the Hadamard projection. If the RFI level is low enough that the common mode signal in the full Hadamard transformation can be sampled, further interference cancellation could be done in digital processing after the Hadamard transformation using the common mode port as an estimator for the RFI. In the case of multiple interferers, the TTD and Hadamard projection can be used to suppress one dominant interferer, and the remainder cancelled in digital processing using (7) with the interferer

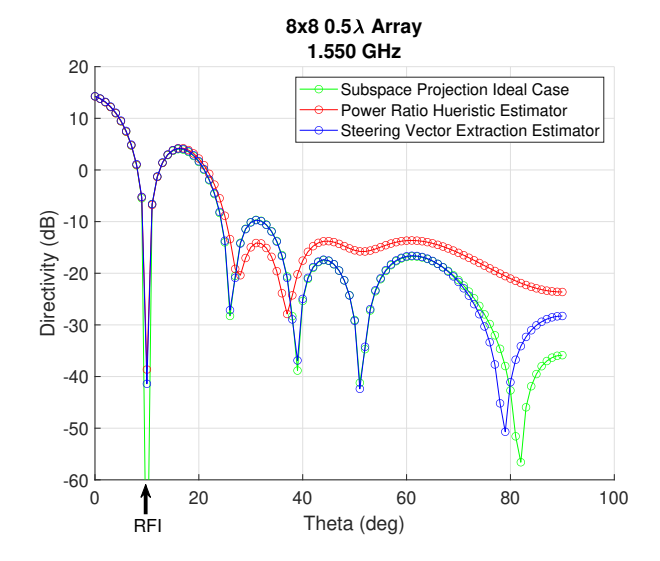


Fig. 6. The residual estimation error obtained after a calibration procedure tends to weaken the null depth and raise side lobe levels. This suggest the effects of non-ideal TTD components will tend to weaken the array pattern.

statistics included in the denominator. In a practical system, temperature drift and other sources of variation mean the TTD calibration may drift. In this case it may be required to use the common mode feedback to adjust the TTD stages and maintain deep nulls on RFI sources.

E. All Digital Implementation

For some situations the native errors in the analog circuitry are intolerable, and a full digital implementation is preferred. With the ever increasing quality of analog converter technology, and the growing capabilities of real time signal processing using FPGAs and GPUs, a real time implementation of the TTD and Hadamard projection can be accomplished computationally. As proved earlier, this method is an alternative implementation of computational wideband subspace projection. An example of a possible digital signal processing architecture for 16 ports is shown in Figure 7.

The linear logarithmic efficiency of traditional channelization stages using the Fast Fourrier Transform manifests in a similar manner using the Fast Hadamard Transform across the full bandwidth. Readers familiar with the Fast Fourier Transform will recognize the similarity of the butterfly steps in the Fast Hadamard Transform. The butterfly operations of the Fast Hadamard Transform can be scheduled efficiently using radix 4 Hadamard kernels (Hadamard matrices of size 4 following the Sylvester construction pattern). The ± 1 structure can be mapped to add/subtract circuits. Several layers of kernels can be chained together to provide an efficient construction of full Hadamard transform (in both analog and digital circuits). Readers familiar with the popular digital circuits implementing the Fast Fourier Transform will be able to see how similar topologies can be used to implement the Fast Hadamard Transform, but without multiplications. Methods of efficiently combining both transforms have been explored in the literature [12] and may prove effective for efficiently combining the first and second stage beamformers.

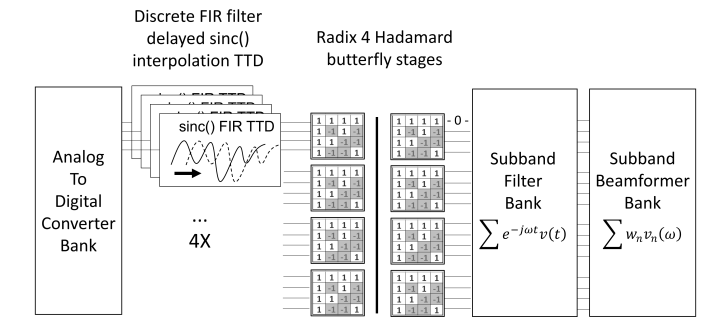


Fig. 7. Example digital architecture of a 16 port implementation of the time delayed Hadamard beamformer and traditional beamforming bank.

Any time delay operation has whole sample delay part plus a fractional delay part with respect to the sample period. The whole part is easily computed via a buffer index shift. The fractional part must be computed by some interpolation scheme between observed sample points. There are many kinds of interpolation algorithms with varying degrees of accuracy and real time computational complexity depending on the SOI bandwidth and noise level. The interested reader may consult the digital signal processing literature for more details on real time signal interpolation. Practical interpolation schemes may require buffering up samples before providing valid input after some latency. This can be modeled by increasing the value of b in (2) to account for the latency.

V. CONCLUSION

This paper has shown that true time delays and Hadamard matrix operators shown in Figure 1 are capable of nulling broadband RFI in aperture arrays from a given spatial direction. It was proven this technique is an isomorphism to the subspace projection beamformer that can easily be implemented in analog circuitry. Unlike other analog beamforming schemes, this method preserves the information to allow synthesis imaging over the full field of view with a secondary digital reconstruction beamformer. The combination allows the ability to recover dynamic range in high sensitivity receivers degraded by RFI. The numerical simulations suggest good performance can be achieved pending the quality of the TTD implementation.

The next step in studying this beamformer is a hardware demonstration based on the results in [3], [4]. This will be reported in a future paper. Applications include protection against co-channel interferers in communication systems, static clutter removal in radar, and reduction of blanked observation due to RFI in passive sensing systems. In view of its structural simplicity, it may be possible to implement the time delayed Hadamard projection method in the digital domain in a way that is more efficient than a bank of traditional narrow band beamformers.

REFERENCES

[1] B. D. Jeffs, K. F. Warnick, J. Landon, J. Waldron, D. Jones, J. R. Fisher, and R. D. Norrod, "Signal processing for phased array feeds in radio astronomical telescopes," *IEEE Journal of Selected Topics in Signal Processing*, vol. 2, no. 5, pp. 635–646, 2008.

- [2] K. F. Warnick, R. Maaskant, M. V. Ivashina, D. B. Davidson, and B. D. Jeffs, *Phased arrays for radio astronomy, remote sensing, and satellite communications*. Cambridge University Press, 2018.
- [3] E. Ghaderi, A. S. Ramani, A. A. Rahimi, D. Heo, S. Shekhar, and S. Gupta, "Four-element wide modulated bandwidth MIMO receiver with 35-dB interference cancellation," *IEEE Transactions on Microwave Theory and Techniques*, vol. 68, no. 9, pp. 3930–3941, 2020.
- [4] —, "An integrated discrete-time delay-compensating technique for large-array beamformers," *IEEE Transactions on Circuits and Systems I: Regular Papers*, vol. 66, no. 9, pp. 3296–3306, 2019.
- [5] R. R. Yarlagadda and J. E. Hershey, "The Hadamard transform and error-correction coding," in *Hadamard Matrix Analysis and Synthesis*. Springer, 1997, pp. 39–50.
- [6] T. K. Moon, Error correction coding: mathematical methods and algorithms. John Wiley & Sons, 2020.
- [7] S. Tahcfulloh and G. Hendrantoro, "Phased-MIMO radar using Hadamard coded signal," in 2016 International Conference on Radar, Antenna, Microwave, Electronics, and Telecommunications (ICRAMET), 2016, pp. 13–16.
- [8] C. Samson, E. Simpson, R. Adamson, and J. A. Brown, "Sparse orthogonal diverging wave imaging on a high-frequency phased array," in 2018 IEEE International Ultrasonics Symposium (IUS), 2018, pp. 1–4.
- [9] G. Zhu and K. Huang, "Analog spatial cancellation for tackling the near-far problem in wirelessly powered communications," *IEEE Journal* on Selected Areas in Communications, vol. 34, no. 12, pp. 3566–3576, 2016
- [10] J. H. Kim and W. S. Park, "A hadamard matrix feed network for a dual-beam forming array antenna," *IEEE Transactions on Antennas and Propagation*, vol. 57, no. 1, pp. 283–286, 2009.
- [11] J. W. Kunzler, K. F. Warnick, M. Chahardori, and D. Heo, "Wideband RFI cancellation using true time delays and a hadamard projection operator," in 2021 IEEE International Symposium on Antennas and Propagation and USNC-URSI Radio Science Meeting, 2021.
- [12] M. T. Hamood and S. Boussakta, "Fast Walsh-Hadamard-Fourier transform algorithm," *IEEE Transactions on Signal Processing*, vol. 59, no. 11, pp. 5627–5631, 2011.



Jakob W. Kunzler Jakob completed his Ph.D. in Electrical and Computer Engineering at Brigham Young University (BYU) in 2022 with funding from the United States Department of Defence's SMART graduate fellowship. He is currently a research scientist at the Naval Information Warfare Center, Atlantic. His interests include antenna technologies, numerical methods, digital communications, radar, FPGA signal processing, and high-performance computing. Jakob is a proud Eagle scout, licensed HAM (KJ7JON), and new father.



Karl F. Warnick Karl F. Warnick (SM'04, F'13) received the B.S. degree in Electrical Engineering and Mathematics and the Ph.D. degree in Electrical Engineering from Brigham Young University (BYU), Provo, UT, in 1994 and 1997, respectively. From 1998 to 2000, he was a Postdoctoral Research Associate and Visiting Assistant Professor in the Center for Computational Electromagnetics at the University of Illinois at Urbana-Champaign. Since 2000, he has been a faculty member in the Department of Electrical and Computer Engineering at

BYU, where he is currently a Professor. Dr. Warnick has published many books, scientific articles and conference papers on electromagnetic theory, numerical methods, antenna applications, and high sensitivity phased arrays for satellite communications and radio astronomy.